

Non-Local Transport Mediated by Spin-Supercurrents

Hua Chen,¹ Andrew D. Kent,² Allan H. MacDonald,¹ and Inti Sodemann¹

¹*Department of Physics, The University of Texas at Austin, Austin, Texas 78712, USA*

²*Department of Physics, New York University, New York, New York 10003, USA*

In thin film ferromagnets with perfect easy-plane anisotropy, the component of total spin perpendicular to the easy plane is a good quantum number and the corresponding spin supercurrent can flow without dissipation. In this Letter we explain how spin supercurrents couple spatially remote spin-mixing vertical transport channels, even when easy-plane anisotropy is imperfect, and discuss the possibility that this effect can be used to fabricate new types of electronic devices.

PACS numbers: 75.76.+j, 75.70.-i, 72.25.Pn, 85.75.-d

Introduction—Recent progress [1] in the growth of magnetic thin films has made it possible to construct circuits in which materials with perpendicular and in-plane magnetic anisotropy are flexibly combined. As we explain below these advances have improved prospects for the experimental realization of a new class of effects in spintronics in which collective magnetic degrees of freedom play a more active role. In this Letter we discuss effects which rely on the ability of ferromagnetic materials with strong easy-plane order to carry dissipationless spin supercurrents [2–6] that are in many ways analogous to the dissipationless charge currents carried by superconductors. In both XY ferromagnets and superconductors the energy of the ordered state is independent of an angle ϕ , the azimuthal magnetic orientation angle in the XY ferromagnet case and the Cooper-pair condensate phase angle in the superconducting case. States with a definite value of this angle break spin-rotational symmetry around the \hat{z} axis and gauge symmetry respectively. The analogy between XY ferromagnetism and superconductivity extends to superflow behavior. Just as superconductors can support dissipationless charge currents, perfect easy-plane ferromagnets can support dissipationless currents [2–6] of the conserved \hat{z} component of total spin.

As an illustration of the types of effects that can occur we address specifically the super-spintronic circuit proposed in Ref. 3 and illustrated in Fig. 1. The circuit consists of two thin film metal stacks containing perpendicular anisotropy magnetic layers and linked by a common easy-plane ferromagnetic thin film, assumed here to be permalloy. As we will describe, collective magnetic behavior induced by exchange interactions within the easy-plane material lead to non-local effects that can be much stronger than the familiar effects associated with spin-diffusion in normal metals. The cross-sectional area of the two stacks and the length of the permalloy link between them are assumed to be sufficiently large to avoid significant charge transport cross-talk [7–9] between stacks. The magnetization of the perpendicularly magnetized metal stacks is assumed to be pinned and only the easy-plane thin film ferromagnet’s magnetization is allowed to change in response to the flow of spin-

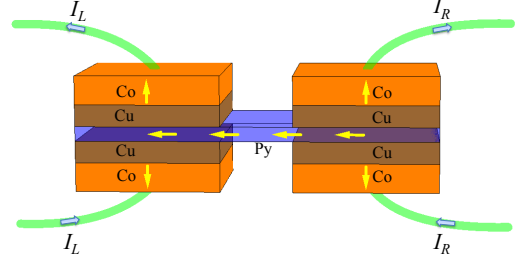


FIG. 1: (color online). Charge transport through two (Left and Right) metallic multilayer stacks containing both perpendicular-anisotropy films and a common easy-plane anisotropy thin film. Transport electrons in both metal stacks exert spin-transfer torques on the easy-plane anisotropy film. Exchange interactions within that film couple the two vertical transport channels. When the orientation of the easy plane ferromagnet is time-independent the left (L) and right (R) conductances are independent. When the total current $I_L + I_R$ exceeds a critical value, spin-transfer torques drive the easy-plane thin-film nano-magnet into a dynamic precessional limit cycle in which the transport properties of the L and R stacks are interdependent. If the Gilbert-damping coefficient of the easy-plane magnet is small, the *dc* conductance of both stacks is strongly suppressed in the dynamic configuration. The specific materials indicated in this illustration are discussed in the text.

polarized currents. The spin-transfer torques exerted by vertical transport drive spin super-currents through the easy-plane nanomagnet. Below we first explain some key ideas by considering simpler macrospin limit in which the spin-stiffness in the thin film nano-magnet is strong enough to inhibit spatial variation in magnetization orientation, and then discuss the long magnetic link limit. **Macrospin Limit**—Because they are separated by non-magnetic spacer layers, the magnetizations of different magnetic circuit elements behave independently. When the system is able to reach a time independent state in the presence of bias voltages, the \hat{z} -direction spin of the easy-plane magnetic layer satisfies the torque-balance equation,

$$\hbar \frac{dS_z}{dt} = -2K \sin(2\phi) + F_L g_L \mu_L + F_R g_R \mu_R = 0, \quad (1)$$

where the first term on the right hand side is contributed

by in-plane magnetic anisotropy, with $-K \cos(2\phi)$ being the macrospin in-plane anisotropy energy. The remaining terms are spin-transfer torques [10, 11] applied at left and right electrodes by number currents

$$I_{L,R} = g_{L,R} \mu_{L,R} / \hbar, \quad (2)$$

where $g_{L,R}$ is the stack conductance in e^2/h units, and $\mu_{L,R}$ the circuit bias energy at the L, R electrode. The currents contribute to dS_z/dt because charge flows between electrodes with opposite perpendicular magnetization orientations; the factors $F_{L,R} \sim 1$ are material-dependent spin-injection efficiency factors, and the conductances $g_{L,R}$ are relatively large because the in-plane nano magnet can efficiently reverse the spins of electrons which propagate through it. Provided that

$$|F_L I_L + F_R I_R| < I_c = 2K/\hbar, \quad (3)$$

Eq. (1) has a solution and the vertical conductance is local in the sense that $I_{L,R}$ depends only on $\mu_{L,R}$. Note that the static solution is allowed for any value of the individual currents as long as the total injected spin-current satisfies Eq. (3).

When the total spin current exceeds $\sim 2K/\hbar$, Eq. (1) can no longer be satisfied. The magnetization can no longer reach a steady state value and begins to precess. Assuming that the easy-plane anisotropy is very large so that the magnetization remains in the XY plane, Eq. (1) then generalizes to

$$\begin{aligned} \hbar \frac{dS_z}{dt} = & -2K \sin(2\phi) - g_i \hbar \dot{\phi} \\ & + F_L g_L (\mu_L - \hbar \dot{\phi}) + F_R g_R (\mu_R - \hbar \dot{\phi}) = 0. \end{aligned} \quad (4)$$

Here the second equality keeps the spin direction close to the easy-plane and the three terms proportional to $\dot{\phi}$ capture magnetization decay due to Gilbert damping and spin-pumping [12, 13] into the two electrodes. The spin-pumping terms can be understood by performing a unitary transformation to a spin-direction frame which precesses with the magnetization. The exchange field of the ferromagnet is then static, allowing standard transport ideas to be applied, but the energy bias across the vertical transport stacks is shifted. In the precessing case

$$\hbar I_{L,R} = g_{L,R} (\mu_{L,R} - \hbar \dot{\phi}). \quad (5)$$

The coefficient g_i in the Gilbert damping term is related to the usual dimensionless damping coefficient α by $\hbar g_i = \alpha S$ where S is the total macrospin of the easy-plane magnetic nano particle.

Given μ_L and μ_R , Eq. (4) can be solved for $\phi(t)$. (Solutions for some typical parameters are presented in Fig. 2.) When the total current is comfortably in excess of the critical value, $\dot{\phi}(t)$ is approximately constant. In this

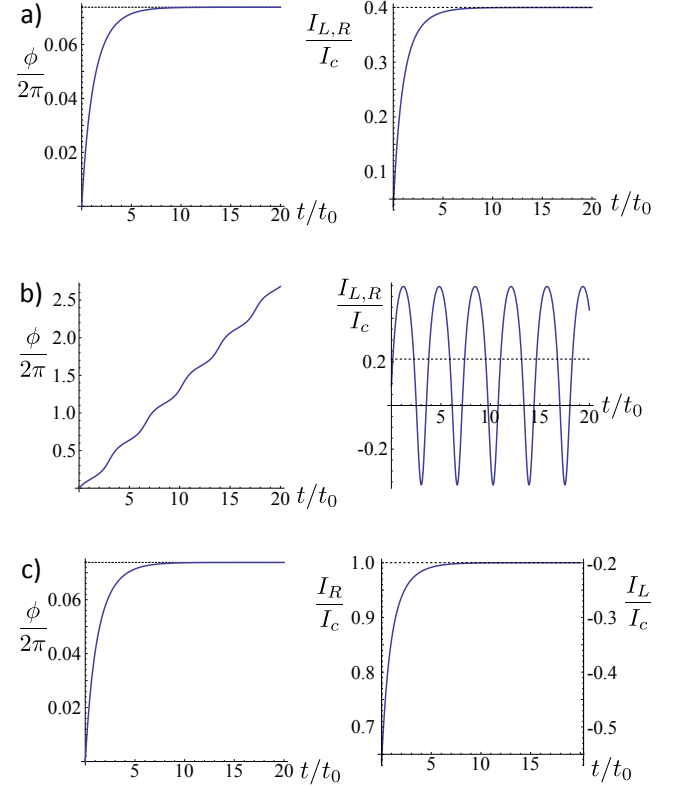


FIG. 2: (color online). Typical Magnetization Dynamics results for $g_i = g_L = g_R = g$, $F_{L,R} = 1$ and initial value $\phi(t=0) = 0$. The left panels depict the evolution of the macro-spin orientation ϕ and the right panels illustrate the behavior of the currents in units of $2K/\hbar$. In each case the dashed line shows the long-time average current. a): $\mu_L = \mu_R = 0.8K/g$ – the total spin-current is below the critical value and the magnetization and currents approach time-independent values. b): $\mu_L = \mu_R = 2.0K/g$ – the total spin current exceeds the critical value. The magnetization precesses non-uniformly and the current has a large oscillating component. The precession becomes more uniform and the oscillating currents weaker when the currents are increased further. c): $\mu_L = -0.4K/g$, $\mu_R = 2.0K/g$ – the spin-current injected by the right contact is the same as in case b) but the total spin-current is the same as in case a). The time unit is $t_0 = \hbar(g_i + g_L + g_R)/(4K)$.

case averaging over time yields the following non-local relationships between electrode currents and biases:

$$\begin{aligned} I_L = & \frac{g_L(g_i + F_R g_R)}{F_L g_L + F_R g_R + g_i} \mu_L + \frac{-F_R g_R g_L}{F_L g_L + F_R g_R + g_i} \mu_R \\ I_R = & \frac{-F_L g_L g_R}{F_L g_L + F_R g_R + g_i} \mu_L + \frac{g_R(g_i + F_L g_L)}{F_L g_L + F_R g_R + g_i} \mu_R \end{aligned} \quad (6)$$

The crossover between Eqs. (2) which apply in the static magnetization regime and Eqs. (6) which apply far into the dynamic magnetization regime occurs rather abruptly as can be seen in Fig. 3 where we plot the time-averaged current in the left electrode I_L vs. μ_L for dif-

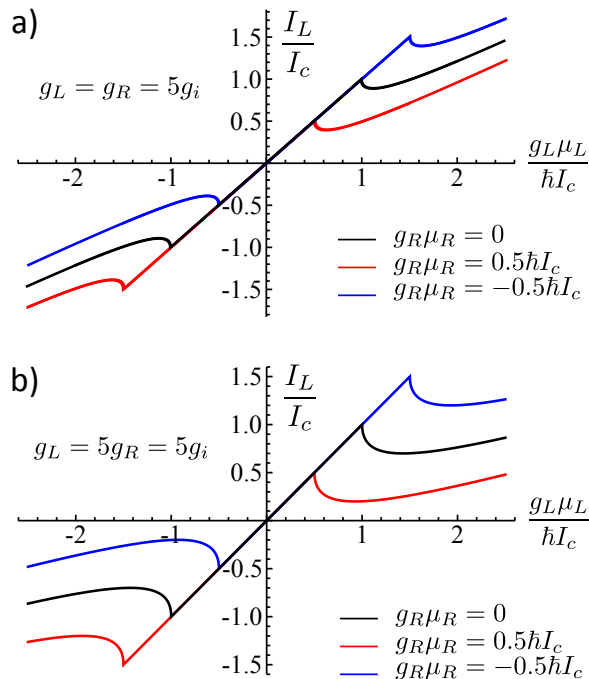


FIG. 3: (color online). Current-voltage relationship of the left electrode for $\mu_R = 0$, $\mu_R = -K/g_R$ and $\mu_R = K/g_R$. Currents in the dynamic regime are time averages over the limit cycle. Panel a) $g_L = g_R = 5g_i$. Panel b) $g_L = 5g_R = 5g_i$. Note that the increase in resistance in the dynamic regime is larger when both g_R and g_i are much smaller than g_L .

ferent values of μ_R .

Both the non-locality of transport and the contrast between the dynamic and static magnetization regimes are enhanced when spin-pumping is the dominant magnetization dissipation mechanism, *i.e.* when $g_{L,R} > g_i$. Achieving sufficiently large spin-injection into easy-plane nano magnets with Gilbert damping that is sufficiently small for this inequality to be satisfied is a challenge which can now be met thanks to recent advances in spin-torque oscillator [14] technology. Because it has a relatively small interface resistance the Co/Cu materials combination is favorable for the perpendicular-magnet/magnetic-spacer elements of the structure. Similarly, because of its small Gilbert damping parameter, permalloy is an attractive material for the easy-plane anisotropy thin film. The Gilbert damping conductance g_i of the permalloy nano magnet is proportional to its total spin and therefore to its volume. The inequality we seek is favored by designing samples in which the easy-plane ferromagnet cross-sectional area is dominated by the portions within the metal stacks and not by the link portion. In this limit $g_{L,R}$ and g_i are both proportional to the stack cross-sectional area, while g_i is in addition proportional to the permalloy thin film thickness. Assuming a Gilbert damping parameter $\alpha \sim 10^{-2}$, and a spin per atom ~ 2 , we conclude that $g_{L,R}$ can be larger than g_i for films thinner than ~ 4 nm. It is of course always possible to

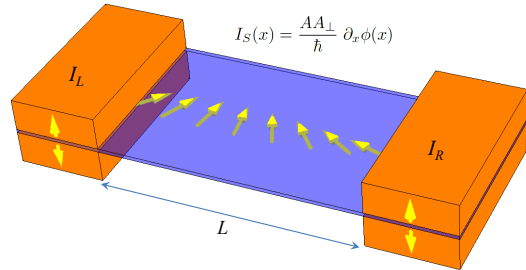


FIG. 4: (color online). Two vertical spin injectors coupled by an easy-plane ferromagnet. The yellow arrows indicate magnetization orientation ϕ within the easy plane. The spin-supercurrent is proportional to the spatial gradient of the magnetization orientation $\partial_x \phi$.

reduce $g_{L,R}$ below maximum values, for example by introducing a thin insulator layer in the metal stacks, to reverse the sense of this inequality in one or both metal stacks. For 1 nm thick films and $\sim 10^{-14}$ m² stack cross-sections, we estimate that $g_{L,R} \leq 300,000$ and, assuming that only 20% of the permalloy area is in the link segment, that $g_i \sim 80,000$. For a given sample shape, the in-plane magnetic anisotropy of thin film permalloy can be controlled by varying growth conditions [15] to values as small as $\sim 10^{-8}$ eV per permalloy spin. It follows that for the same device dimensions, the bias energies necessary to drive the transition between static and dynamic regimes can be as small as $\sim 10^{-7}$ eV. Electronic transport switches which operate at such small bias voltages are potentially attractive for low-power-consumption electronic devices.

Long Nanomagnet Limit— When the in-plane magnetic anisotropy is tuned to larger values, spatial variation of the magnetization orientation can become important. In Fig. 4 we illustrate the case of a long narrow permalloy thin film which provides a magnetic link between metal electrodes at left and right. Assuming that the link is sufficiently narrow to force constant magnetization across the bar, the Landau-Lifshitz equation in this case is

$$-2\frac{K}{L}\sin(2\phi) - \frac{g_i}{L}\hbar\dot{\phi} + AA_{\perp}\partial_x^2\phi = 0, \quad (7)$$

where A_{\perp} is the cross-sectional area of the bar, L is its length, and A is the magnetic stiffness coefficient. The two terms that are balanced in the static limit can be interpreted as contributions to the rate of change of the local S_z density from local magnetization precession and from the divergence of the spin-supercurrent,

$$I_S(x) = \frac{AA_{\perp}}{\hbar}\partial_x\phi(x). \quad (8)$$

Because the exchange splitting of typical ferromagnetic metals is much larger than the anisotropy energy per particle, the spin-current injected at left and right is converted [16, 17] nearly locally into a spin-supercurrent. It

follows that

$$\begin{aligned} I_S(x=0) &= F_L I_L = F_L g_L [\mu_L - \hbar \dot{\phi}(x=0)], \\ I_S(x=L) &= -F_R I_R = -F_R g_R [\mu_R - \hbar \dot{\phi}(x=L)]. \end{aligned} \quad (9)$$

As in the macrospin limit vertical transport at each electrode is local when the easy-plane magnetization orientation is static, but the switching boundary is dependent on both bias voltages. Some insight into switching properties can be gained by noting that in the static case

$$\frac{\hbar^2 I_s^2}{2AA_\perp} + \frac{K}{L} \cos(2\phi) = C, \quad (10)$$

where C is a constant independent of position. When $F_L I_L = -F_R I_R$ the spin-supercurrent has the same value at L and R bar ends, and static magnetization configurations are allowed at large current magnitudes. When I_L and I_R have the same sign at the bar ends, however, I_s must change sign as a function of position along the bar and static solutions are possible only when:

$$\max(F_L^2 I_L^2, F_R^2 I_R^2) < \frac{4KAA_\perp}{L\hbar^2}. \quad (11)$$

For large K this limit on the injected spin-currents is more stringent than Eq. 3. In both cases the spin-injection limit depends on bias voltages in both metal stacks and the collective magnetic degree of freedom provides the coupling between electrodes.

The ratio of the length of the permalloy link, L , to the typical magnetization variation length scale:

$$\lambda \equiv \frac{1}{2} \sqrt{\frac{AA_\perp L}{K}}, \quad (12)$$

controls how far the system is from the macrospin limit. When $L \ll \lambda$ the critical currents are given by the macrospin result in Eq. (3). In the opposite limit, $L \gg \lambda$, the currents at which steady solutions exist satisfy Eq. (11) except within a narrow strip along the $F_R I_R = -F_L I_L$ line. Figure 5 illustrates this behavior.

Discussion— The I-V characteristics discussed in this Letter provide an example of an electron transport phenomenon in which a collective degree-of-freedom, the magnetization orientation, plays an active role. This type of phenomenon is of potential interest for electronic device applications mainly because it can lead to current flow response to bias voltage that is sharp on scales smaller than $k_B T/e$, an impossibility for the single-particle transport processes exploited in most current electronic devices. We have so far ignored the role of thermal fluctuations in the phenomena discussed here. Switching between static and dynamic magnetization configurations [18–20] is stochastic with a thermal energy barrier due to anisotropy that vanishes at the critical currents or bias voltages. It follows that reliable collective switching can be driven by changes in bias voltage

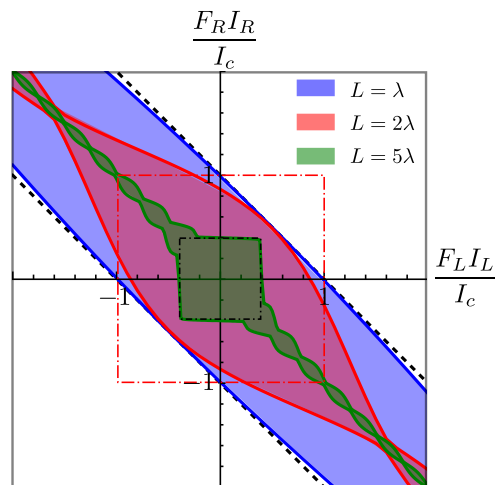


FIG. 5: (color online). Regions in the $I_{L,R}$ parameter space where static magnetization solutions exist. The blue, red, and green regions correspond to different ratios of the permalloy link length, L , to the length λ defined in Eq. (12). The dashed black lines enclose the region predicted by Eq. (3) intended to apply in the macrospin model. The box enclosing the entire picture, the red dashed-dotted box and the black dashed-dotted box enclose the regions described by Eq. (11), intended to apply in the long-link limit, for $L = \lambda$, $L = 2\lambda$, $L = 5\lambda$ respectively. Note that the $L = \lambda$ case (blue region) is already well described by the macrospin model, whereas the $L = 5\lambda$ (green region) is already well described by Eq. (11), except for a narrow strip near $F_R I_R = -F_L I_L$.

δV with $e\delta V/k_B T \sim eV_{\text{switch}}/K \sim 1/g_{L,R} \ll 1$, where V_{switch} is the bias voltage typically required for switching, exceeding the limit possible with switches based upon individual independent electron behavior.

Acknowledgements.— HC, IS and AHM were supported by the Welch Foundation under Grant No. TBF1473 and by the SWAN nano electronics program. ADK was supported by NSF-DMR-1309202 and the SRC-INDEX spin logic program.

-
- [1] A. Brataas, A. D. Kent, and H. Ohno, Nature Materials **11**, 372 (2012).
 - [2] For a review of theoretical work on this topics, which has a rather long history, see E.B. Sonin, J. Low Temp. Physics **171**, 757 (2013) and work cited therein.
 - [3] Jürgen König, Martin Chr. Bønsager, and A. H. MacDonald, Phys. Rev. Lett. **87**, 187202 (2001).
 - [4] F. S. Nogueira and K.-H. Bennemann, Europhys. Lett. **67**, 620 (2004).
 - [5] S. Takei and Y. Tserkovnyak, Phys. Rev. Lett. **112**, 227201 (2014).
 - [6] S. Takei, B. I. Halperin, A. Yacoby, and Y. Tserkovnyak, arXiv:1404.3987.
 - [7] The resistance of 1 nm thick permalloy thin films at room temperature is [8] $\sim 300 \Omega$ per square. The resistance area product of the Co/Cu metal stacks is typically near $10^{-15} \Omega\text{m}^2$ [9]. For a permalloy link widths of $\sim 5 \times$

- 10^{-8} m, and a lateral dimensions of the metal stacks of $\sim 10^{-7}$ m, the link resistance ($\sim 500 \Omega$) is substantially larger than the stack resistance ($\sim 0.1 \Omega$). Crosstalk has little influence on device performance unless the stack resistance is comparable to the link resistance.
- [8] A.F. Mayadas, J.F. Janak, and A. Gangulee, *J. Appl. Phys.* **45**, 2780 (1974).
- [9] J. Bass and W.P. Pratt Jr., *J. Mag. Mag. Mater.* **200**, 274 (1999).
- [10] J. C. Slonczewski, *J. Mag. Mag. Mat.* **159**, L1-L7 (1996); M. Tsoi, A. Jansen, J. Bass, W.-C. Chiang, M. Seck, V. Tsoi and P. Wyder, *Phys. Rev. Lett.* **80**, 4281 (1998); E. Myers, D. Ralph, J. Katine, R. Louie and R. Buhrman, *Science* **285**, 867-870 (1999); J. Sun, *J. Mag. Mag. Mat.* **202**, 157-162 (1999).
- [11] D. C. Ralph and M. D. Stiles, *J. Mag. Mag. Mat.* **320**, 1190 (2008).
- [12] Y. Tserkovnyak, A. Brataas, G.E.W. Bauer, and B.I. Halperin, *Rev. Mod. Phys.* **77**, 1375 (2005).
- [13] We have for simplicity assumed that the efficiency factors are identical for spin-transfer torques and spin-pumping. This is strictly speaking true only when the source and drain electrodes are fully spin selective.
- [14] S.I. Kiselev, J.C. Sankey, I.N. Krivorotov, N.C. Emley, R.J. Schoelkopf, R.A. Buhrman, and D.C. Ralph, *Nature* **425**, 380 (2003); W.H. Rippard, M.R. Pufall, S. Kaka, S.E. Russek, and T.J. Silva, *Phys. Rev. Lett.* **92**, 027201 (2004).
- [15] Alfredo Garcia-Arribas, Eduardo Fernandez, Andrey V. Svalov, Galina V. Kurlyandskaya, Ane Barrainkua, David Navas, and Jose Manuel Barandiaran, *Eur. Phys. J. B* **86**, 136 (2013); A. Garcia-Arribas, E. Fernandez, I. Orue, and J. M. Barandiaran, *Appl. Phys. Lett.*, **103**, 142411 (2013).
- [16] Hua Chen, Inti Sodemann, and A.H. MacDonald, to be published (2014).
- [17] Jung-Jung Su and A.H. MacDonald, *Nature Physics*, **4**, 799 (2008).
- [18] R. H. Koch, J. A. Katine, and J. Z. Sun, *Phys. Rev. Lett.* **92**, 088302 (2004).
- [19] I. N. Krivorotov, N. C. Emley, A.G. F. Garcia, J.C. Sankey, S. I. Kiselev, D. C. Ralph, and R. A. Buhrman, *Phys. Rev. Lett.* **93**, 166603 (2004).
- [20] V. Ambegaokar and B.I. Halperin, *Phys. Rev. Lett.* **22**, 1364 (1969).